Catal Lett (2008) 121:297–302
DOI 10.1007/s10562-007-9337-9

In Situ Preparation of Functional Heterogeneous Organotin Catalyst Tethered on SBA-15

Binbin Fan · Jilong Zhang · Ruifeng Li · Weibin Fan

Received: 10 September 2007 / Accepted: 31 October 2007 / Published online: 15 November 2007

Abstract A stable heterogeneous organotin catalyst has been prepared by in situ tethering organotin compounds on SBA-15. This was verified by XRD, TEM, N_2 adsorption/desorption at −196 °C, FTIR and diffuse reflectance UV–vis spectral techniques. This material was much more active than the sample prepared by the grafting method for the direct synthesis of dimethyl carbonate (DMC) from methanol and CO_2 despite that its catalytic activity was dependent on the organotin amount. This could be attributed to the formation of organotin clusters with different structures and the larger surface area. After immobilization on the SBA-15 mesoporous material, the six-coordinated organotin clusters showed higher activity, compared to the tetrahedral Sn species. With increasing reaction temperature and CO_2 pressure, the catalytic activity considerably increased.

Keywords Carbon oxide · Dimethyl carbonate · Heterogeneous catalysis · Organotin · SBA-15

1 Introduction

Organotin compounds have been proved to be industrially important as an effective stabilizer in polyvinyl chloride (PVC) and good biocides and pesticides [1]. These materials could also act as catalysts for organic synthesis such as production of polyurethane foams and electrocoat (E-coat) coatings. In addition, it was shown that organotin compounds such as distannanes could catalyze the reaction of direct synthesis of dimethyl carbonate (DMC) from CO_2 and methanol [2–5]. This process gains much interest because of its environmentally benign character and the versatility of DMC as an attractive eco-friendly alternative to both methyl halides (or dimethyl sulfate) and phosgene in methylation and carbonylation processes, respectively [6], and as a fuel additive [2–5].

However, organotin compounds are highly toxic as a result of mutation of gene, aberration of chromosome or formation of mammalian erythrocyte micronucleus [1]. In particular, these compounds could repeatedly dose toxicity and reproduce toxicity through fertilization and development. Removal of organotin is also very difficult because of its ready hydrolysis, photodegradation, biodegradation and fugacity. In view of sustainable and green chemistry, heterogenization of organotin in the way of encapsulation/immobilization of transition metal complexes in the host matrixes such as zeolites and mesoporous materials [7–12] would be desirable because this could make catalyst separation easy and allow further recovering and reusing the catalyst. In this aspect, organotin compounds have been anchored on the polymer and polyoxotungstates [13, 14], both of which, however, have poor mechanical and limited thermal stability, leading to the leaching of tin [15]. It is interesting that organotin hydrides recently have been grafted on inorganic oxides such as SiO_2, Al_2O_3, ZrO_2 and TiO_2 [15], but the surface area of these supports are small, resulting in a much lower conversion than the polymer supported analogue in the reduction of 1-iodoocane to *n*-octane. Mesoporous silica has a uniform structure with very large OH-rich surface area and tunable pore size in the

B. Fan · J. Zhang · R. Li
Institute of Special Chemicals, Taiyuan University of Technology, 79 West Yingze Street, Taiyuan 030024, China

W. Fan (✉)
State Key Laboratory of Coal Conversion, Shanxi Institute of Coal Chemistry, Chinese Academy of Sciences, 27 South Taoyuan Road, Taiyuan 030001, China
e-mail: fanwb@sxicc.ac.cn

range of 2–30 nm. A successful immobilization of organotin compounds on the mesostructured silica would create new organotin/inorganic hybrid materials with high thermal and mechanical stability as well as large surface area and controlled porosity. Here, we report the in situ preparation of functional heterogeneous organotin catalyst tethered on SBA-15, and the prepared material shows significantly improved catalytic performance for the direct synthesis of DMC from methanol and CO_2.

2 Experimental

2.1 Synthesis of $(MeO)_2ClSi(CH_2)_3SnCl_3$

*2.1.1 Synthesis of 1,1-Dichloro-1-silacyclobutane (**1**)*

1 was synthesized according to the method reported by Laane [16]. About 20.4 g of magnesium was first put in a two-neck round bottom flask (2 L) equipped with a condenser and a heater. Then, 250 mL of ethyl ether was added together with a small amount of iodine. This was followed by the dropwise addition of 108 g of (3-chloropropyl)trichlorosilane within 8 h under stirring and gentle refluxing conditions. The resultant slurry was continued to reflux for 30 h. After adding another 20 g of magnesium and 600–700 mL of ethyl ether, a further reflux of 3 days was performed. Finally, white $MgCl_2$ and excessive Mg turnings were filtered and washed several times with ethyl ether. The filtrate was then distilled to obtain 60 g of **1** with a yield of 88%. ^{1}H NMR (300 MHz, $CDCl_3$): δ 2.0–2.2 (m, 2H), 1.8–2.0 (m, 4H). ^{13}C NMR (75.5 MHz, $CDCl_3$): δC_α 27.2, C_β 14.0. ^{29}Si NMR (59.6 MHz, $CDCl_3$): δ 17.7.

*2.1.2 Synthesis of 1,1-Dimethoxy-1-silacyclobutane (**2**)*

2 was synthesized with a modified method described in a US patent (3,687,995). Typically, 7.53 g of trimethyl orthoformate was dropwise added to 5 g of **1** at 0 °C under stirring conditions. Then, the reaction was carried out at 80 °C for 4 h. After removal of CH_3Cl and $HCO(OCH_3)$, **2** was obtained. ^{13}C NMR (75.5 MHz, $CDCl_3$): δ C_α 19.4, C_β 11.0, methoxyl 49.6. ^{29}Si NMR (59.6 MHz, $CDCl_3$): δ −13.2.

*2.1.3 Synthesis of $(MeO)_2ClSi(CH_2)_3SnCl_3$ (**3**)*

Synthesis of **3** was conducted on the basis of a US patent (6,506,918). To 1.43 g of **2** and 8 mL of toluene was dropwise added 4.45 g of $SnCl_4$ at 0 °C, which was then stirred at room temperatures for 2 days. This was followed by a reflux of 6 h to form **3**. **3** was purified by distilling solvent at 100 °C under vacuum conditions. ^{29}Si NMR (59.6 MHz, $CDCl_3$): δ −28.9.

*2.1.4 Synthesis of Samples with **3** Tethered on SBA-15*

The sample was synthesized with tetraethyl orthosilicate (TEOS), Pluronic 123 (P123), hydrochloric acid (HCl), distilled water and $(MeO)_2ClSi(CH_2)_3SnCl_3$ (**3**) according to the composition of $6.1HCl:(1-x)TEOS:x(MeO)_2ClSi(CH_2)_3SnCl_3:0.017P123:165H_2O$ ($x = 0$–0.1). For a typical synthesis, 4 g P123 was first dissolved in 125 g HCl aqueous solution (2 mol/L) at room temperature. To this solution was added the required amount of TEOS. Then, it was heated at 40 °C for 3 h under stirring conditions. This was followed by the slow addition of **3**. The resultant mixture was further agitated at 40 °C for 1 h and statically kept at 100 °C for 48 h. The solid product was filtered, washed with deionized water and dried at ambient temperature. Removal of surfactant was conducted by refluxing the sample in ethanol for 48 h. The extracted sample was dried at 50 °C under vacuum conditions.

2.2 Characterization of Samples

Powder X-ray diffraction patterns (XRD) were recorded on a Rigaku D/Max-2500 diffractometer (40 kV, 40 mA) with CuKα radiation. TEM images were collected on a JEM 2010 transmission electron microscope at an acceleration voltage of 120 kV. N_2 adsorption/desorption measurements were carried out at −196 °C on a Quantachrone Autosorb Chemisorption-physisorption analyzer. Before the measurement, the sample was evacuated at 200 °C for half hour. The BET surface area was calculated from the adsorption branch in the range from 0.05 to 0.25, while the pore volume was estimated at a relative pressure of 0.99. The pore size was evaluated from the desorption branch with Barrett–Joyner–Halenda (BJH) method. FTIR spectra were collected on a Shimadzu FTIR 8010 spectrometer by using conventional KBr pellet method. Diffuse reflectance (DR) UV–vis spectra were measured on a Perkin-Elmer Lambda Bio40 UV–vis spectrophotometer equipped with an integration sphere. The liquid NMR spectra were recorded on a Bruker DRX 300 nuclear magnetic resonance spectrometer, while the solid MAS NMR measurements were performed on a VARIAN^{unity} INOVA nuclear magnetic resonance spectrometer (300 MHz). The spinning rate of the rotor was 5 KHz. A pulse length of 1.5 μs was applied and about 24,000 scans were accumulated with a repetition time of 3 s. Sn content was determined by an inductively coupled plasma-atomic emission spectrometer (ICP-AES) (Atomscan 16, TJA Corporation).

2.3 Catalytic Measurements

Direct synthesis of dimethyl carbonate (DMC) from methanol and carbon dioxide was conducted in a 100-mL stainless steel batch reactor (Parr) equipped with a thermal couple, a magnetic stirrer and a heater. Typical reaction conditions are as follows: 0.1 g catalyst, 0.49 mol methanol, a CO_2 pressure of 180 atm, 200 °C, 10 h. The product was analyzed with a GC7890 gas chromatographer equipped with a SE-30 (60 m in length) capillary column and a flame ionization detector.

3 Results and Discussion

Table 1 gives the sample notations (Sn_y-SBA-15 with y representing 1000×), Sn content and the physical properties of the extracted samples. Figure 1 shows the XRD patterns of the samples synthesized with the gels having different contents of $(MeO)_2ClSi(CH_2)_3SnCl_3$ (**3**). Clearly, all samples exhibited three sharp diffraction lines, which could be indexed to (100), (110) and (200) reflections. This is indicative of a highly ordered hexagonal array of the formed structure. This is further substantiated by the commonality of TEM images of the extracted samples for typical hexagonal symmetry (Fig. 2). Nevertheless, the gradual ill-resolved (110) and (200) reflections with increasing content of **3** in the synthesis gel imply a decrease in the ordering of the hexagonal symmetry.

N_2 adsorption/desorption isotherms at −196 °C are shown in Fig. 3. A typical type IV isotherm with a H1 hysteresis loop was observed for all the samples, evidencing that the prepared materials have a mesoporous structure irrespective of the amount of the organotin compound added to the synthesis gel. Nevertheless, the BET surface area and pore volume decreased with the content of **3** in the gel, revealing the presence of more **3** in the pores. The narrow pore size distribution calculated from the desorption branch by BJH method indicates a homogeneous distribution of **3** in the samples. The pore diameter varied from 8.2 to 4.8 nm, depending on the **3** amount. This is consistent with the results obtained through TEM image analyses.

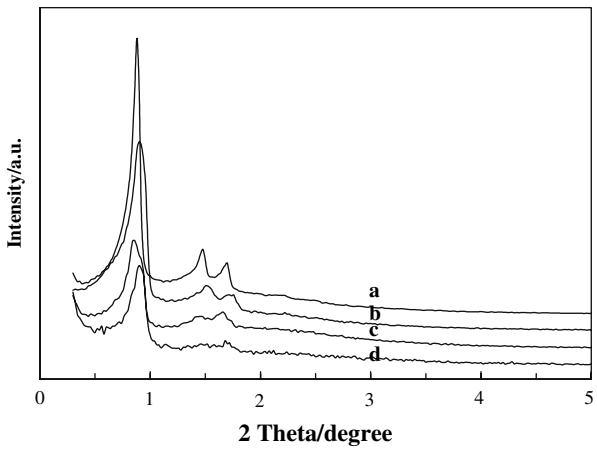

Fig. 1 XRD patterns of the (a) Sn_{14}-SBA-15, (b) Sn_{20}-SBA-15, (c) Sn_{54}-SBA-15 and (d) Sn_{85}-SBA-15 samples

One question that has to be answered is whether the organotin **3** was immobilized on the SBA-15. ICP analyses show that the Sn amount in the prepared samples monotonically increased with increasing content of **3** in the synthesis gel (Table 1), revealing that about 35–55% of **3** added to the synthesis gel attached to the SBA-15. The homogeneous distribution of **3** in the samples is further verified by energy dispersion X-ray (EDX) analysis, which shows as an example that the Sn contents in the different crystals of the Sn_{54}-SBA-15 sample were all about 6.4 wt.%, in a good agreement with the bulk analysis. The absorbance bands attributed to the C–H stretching and bending vibrations were observed at 2,985, 2,940 and 1,461 cm^{-1} in the IR spectra (Fig. 4A). In contrast, the bands, characteristic of Sn–O(Py)–Sn (Py = propyl) and Si–O(Py)–Sn, at about 800 and 960 cm^{-1} were overlapped by the Si–O stretching vibration of tetrahedral SiO_4 and the Si–OH vibration in defect sites respectively [17, 18]. This is suggested by the increase in intensity of the band around 674 cm^{-1}, ascribed to Sn–O–(Si) and Sn–O(Py or H)–Sn vibrations [17], with increasing Sn content. ^{13}C CP MAS

Table 1 Chemical compositions, physical properties and catalytic data of the prepared catalysts

Sample	X[a]	Sn amount (mmol g^{-1})	a	BET surface area (m^2 g^{-1})	Pore diameter (nm)	Pore volume (mL g^{-1})	TON[b]
Sn_{85}-SBA-15	0.085	0.72	11.20	547	4.76	0.73	1.9
Sn_{54}-SBA-15	0.054	0.52	11.33	582	5.23	0.75	2.3
Sn_{20}-SBA-15	0.020	0.11	11.85	593	5.69	0.87	2.7
Sn_{14}-SBA-15	0.014	0.09	11.58	752	8.19	1.01	3.0
Sn_{64}/SBA-15	–	0.64	–	475	6.75	0.60	1.3

[a] The chemical compositions of the gel: 6.1HCl:(1 - x)TEOS:$x$$(MeO)_2ClSi(CH_2)_3SnCl_3$:0.017P123:165$H_2O$

[b] Reaction conditions: 0.1 g of catalyst, 0.49 mole of methanol, CO_2 pressure of 180 atm, 200 °C, 10 h

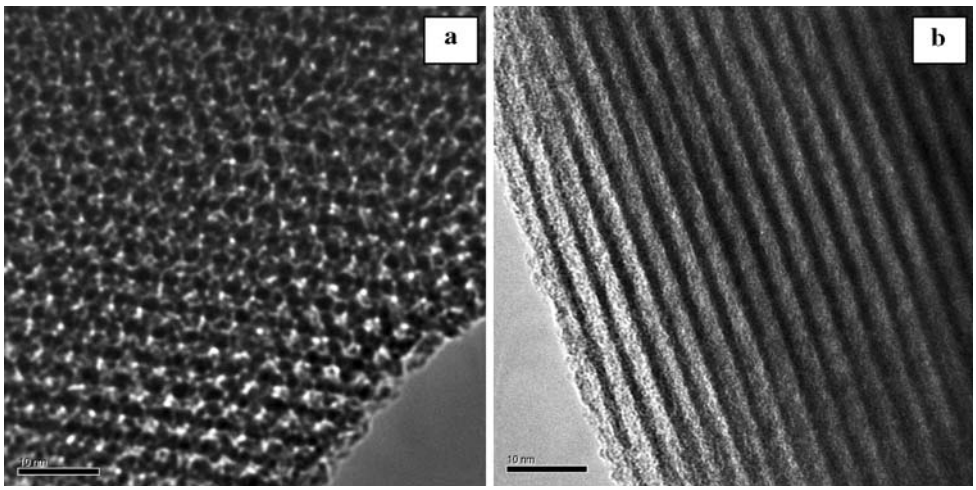

Fig. 2 TEM images of the Sn_{54}-SBA-15 sample along (**a**) (100) and (**b**) (110) incidences (scale bar: 10 nm)

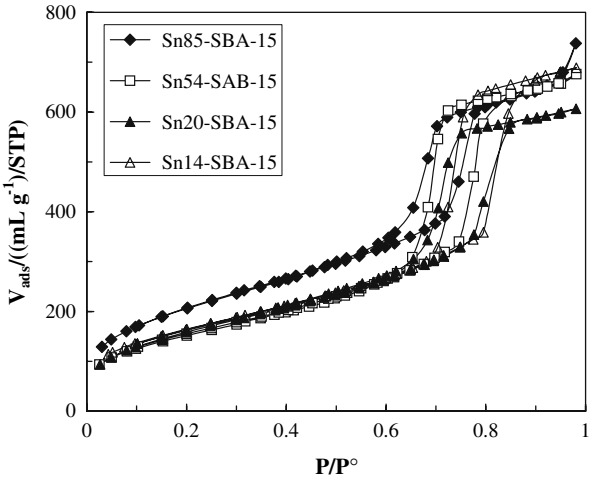

Fig. 3 N_2 adsorption/desorption isotherms at −196 °C of the prepared catalysts

NMR shows an intense peak at 18 ppm (not shown here), which is due to the propyl group directly bonded to Si atoms [19]. This evidences the non-cleavage of **3** during synthesis. The above characterization results show that **3** was present in the prepared catalysts, in accordance with XRD and N_2 adsorption/desorption measurements.

Another important question is what the state of **3** is in the prepared catalysts. As we know, monoalkyltin compounds exhibit a rich oxo-cluster chemistry based on Sn–O(S)–Sn [20, 21]. The formed cluster structure depends on the alkyl, solvent, Sn content and solvolysis conditions [20]. Thus, hydrolysis of organotin provides another way to synthesize oxo-hydroxo species with different structures [21], which could be further interconverted [20]. Up to date, the structures of most clusters have not been solved yet because of their profound complexity. Irrespective of this, Sn ions usually have a coordination number of six. This is consistent with our experimental result that two bands around 252 and 285 nm (Fig. 4B), assigned to the small and polymeric hexa-coordinated Sn species respectively [22], were observed in the DR UV–vis spectra of the extracted samples such as the Sn_{54}-SBA-15. This suggests that at least two types of clusters were formed. The formation of organotin cluster is also supported by the presence of the band attributable to Sn–O(Py or H)–Sn vibration in the IR spectra. Although the exact cluster structure was not clear for a moment, the EDX analysis reveals that the Sn/Cl molar ratio was about 10 in the prepared Sn_{54}-SBA-15 catalyst. In addition, the absence of a band above 300 nm in the DR UV–vis spectra shows that the formed organotin clusters is free of SnO_2 and materials with a structure analogous to SnO_2 [23].

The similar unit-cell parameters ($a = 2d_{100}/(3^{1/2})$) of the samples containing different amounts of organotin indicate that the organotin was not incorporated in the framework as a bridge but immobilized on the pore wall of SBA-15 (Table 1). Indeed, it was shown by ^{29}Si MAS NMR that besides the lines assigned to Q^4 (−110 ppm), Q^3 (−101 ppm) and Q^2 (−92 ppm), one line centered at −79 ppm was observed for the organotin-containing samples, whereas it was absent for the pure silica SBA-15 (Fig. 4C). This line is attributed to T^3 ($(SiO)_3Si$–C) [24, 25], proving that organotin was successfully tethered on the SBA-15 during the synthesis process. Since no T^1 and T^2 species was detected, it could be deduced that hydrolysis of **3** is complete, probably leading to a stable joint between the pore wall and the formed organotin cluster.

The direct synthesis of DMC from methanol and CO_2 is a thermodynamically controlled reaction. To eliminate the effect of kinetics and understand well the catalytic performance of different organotin compounds, Table 1 shows the turnover number (TON, the amount of formed DMC per mole of Sn ions) obtained at the reaction time of 10 h in order that it can be assured that the DMC yield almost linearly increases with the reaction time. Obviously, the

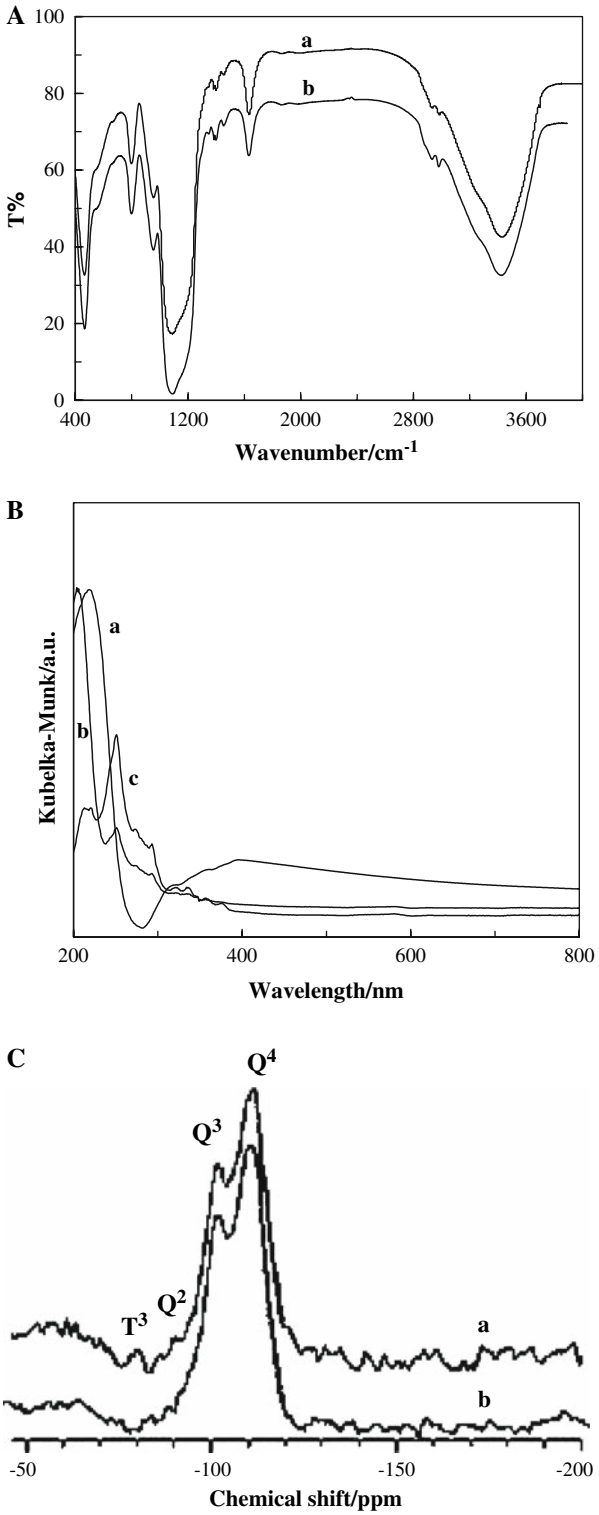

Fig. 4 (**A**) IR spectra of the (**a**) Sn_{85}-SBA-15 and (**b**) Sn_{54}-SBA-15 samples; (**B**) DR UV–vis spectra of the (**a**) Sn_{64}/SBA-15 (prepared by the grafting method), (**b**) Sn_{85}-SBA-15 and (**c**) Sn_{54}-SBA-15 samples; (**C**) ^{29}Si MAS NMR spectra of the (**a**) Sn_{85}-SBA-15 and (**b**) pure silica SBA-15 samples

TON monotonically increased with decreasing Sn content in the prepared samples. The TON for the Sn_{85}-SBA-15 sample was 1.9, while it increased to 3.0 for the Sn_{14}-SBA-15. Regardless of this, the Sn_{64}/SBA-15 prepared by using the grafting method with a Sn content of 0.64 mmol g^{-1} only gave a TON of 1.3. This is perhaps due to the different structures of the organotin clusters formed in the different samples, as indicated by DR UV–vis spectroscopy (Fig. 4 B). The Sn_{64}/SBA-15 showed one intense band at 215 nm, which is due to the electronic transition from O^{2-} (ligand) to Sn^{4+} of highly dispersed tetrahedral Sn species [22, 23]. In contrast, hexa-coordinated Sn clusters were primarily present in the Sn_{54}-SBA-15 sample, as shown by the fact that the bands at 252 and 285 nm were much more intense than the band at 210 nm. The formation of organotin clusters through hydrolysis depends on the concentration of organotin monomer in the synthesis gel of SBA-15 [20]. The low concentration of **3** resulted in the formation of major organotin clusters, whereas high content gave mainly tetra-coordinated Sn species irrespective of the presence of a small amount of hexa-coordinated Sn clusters (curves b and c in Fig. 4B). This suggests that organotin clusters with Sn species having a coordination number of six might promote the carbonation of alcohol much more than tetra-coordinated Sn-containing organotin species. In addition, the large surface area of the samples with a low content of organotin would make the active sites more accessible to the reactants. As a result, in situ synthesized Sn_y-SBA samples exhibited higher catalytic activity than the Sn_z/SBA-15 prepared by the grafting method, and the activity increased with decreasing Sn content.

Figure 5 shows that the catalytic activity monotonically increased with increasing CO_2 pressure, as revealed by the gradual increase in TON obtained over the Sn_{85}-SBA-15 sample. This could be accounted for from the thermodynamics and kinetics. The direct synthesis of DMC from methanol and CO_2 is a volume-decreased reaction. This leads to a progressive decrease in the overall pressure with the proceeding of the reaction. Thus, a high CO_2 pressure would push the reaction towards the formation of DMC before the thermodynamic balance is reached. In particular, a high CO_2 pressure would make the reaction mixture more homogeneous as a result of the formation of supercritical CO_2 medium when the pressure reaches 200 atm [3], causing a gradual change from biphase to monophase, and thus, an increased CO_2 density in the liquid fraction with increasing CO_2 pressure [26]. This would strongly promote the reaction. As expected, an increase in the reaction temperature significantly improved the catalytic performance within the kinetically controlled region. Under the

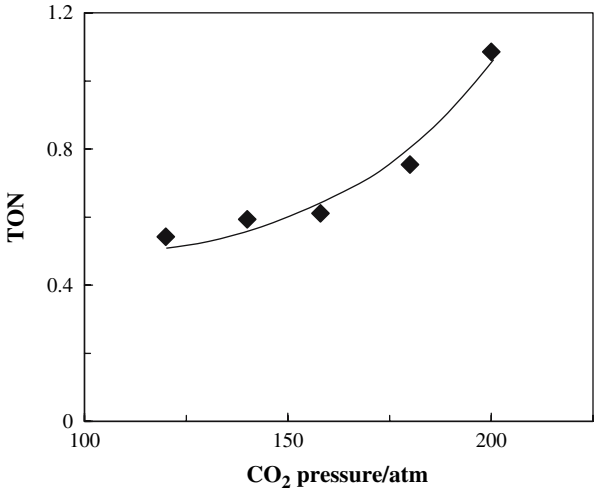

Fig. 5 Dependence of the catalytic activity of Sn_{85}-SBA-15 on the CO_2 pressure (Reaction conditions: 0.1 g of catalyst, 0.49 mole of methanol, 183 °C, 10 h)

same CO_2 pressure of 180 atm and the reaction time of 10 h, the TON obtained at 240 °C over the Sn_{85}-SBA-15 was 2.43 in contrast to 0.75 attained at 180 °C.

It is noteworthy that the prepared Sn_y-SBA-15 catalysts exhibited high stability against leaching, as substantiated by ICP analysis result that no Sn species was detected in the reaction mixture. As an example, within five repeated runs, the TON obtained on the Sn_{20}-SBA-15 sample with regeneration (after one run, the catalyst was filtered and washed with methanol, and then dried at 60 °C under vacuum conditions for next run) was between 2.6 and 3.0 under the reaction conditions shown in the footnote of Table 1, confirming that the prepared Sn_y-SBA-15 material is a reusable and environmentally benign heterogeneous catalyst.

4 Conclusions

A new functional heterogeneous organotin catalyst has been prepared by in situ tethering organotin compound on the pore wall during the synthesis of SBA-15. This material shows much higher activity than the sample prepared by the grafting method in the direct synthesis of DMC from methanol and CO_2 as a result of the formation of organotin clusters with different structures and possessing a larger surface area. The hexa-coordinated Sn clusters are more active than the tetrahedral Sn species. The high stability against leaching during the reaction process evidences the truly heterogeneous catalytic character of Sn_y-SBA-15. This would greatly reduce the organotin pollution. An increase in the CO_2 pressure and the reaction temperature significantly improves the catalytic performance.

Acknowledgments This work is supported by the National Science Foundation of China (No. 20301012). W. F. gratefully thanks the support of "Hundred Talents" project of the Chinese Academy of Sciences.

References

1. Batt JM (2005) Appl Organometal Chem 19:458
2. Ballivet-Tkatchenko D, Jerphagnon T, Ligabue R, Plasseraud L, Poinsot D (2003) Appl Catal A 255:93
3. Ballivet-Tkatchenko D, Chambrey S, Keiski R, Ligabue R, Plasseraud L, Richard P, Turunen H (2006) Catal Today 115:80
4. Ballivet-Tkatchenko D, Douteau O, Stutzmann S (2000) Organometallics 19:4563
5. Choi J, He L, Yasuda H, Sakakura T (2002) Green Chem 4:230
6. Tundo P, Selva M (2002) Acc Chem Res 35:706
7. Ernst S, Fuchs E, Yang X (2000) Microporous Mesoporous Mater 35–36:137
8. Ernst S, Disteldorf H, Yang X (1998) Microporous Mesoporous Mater 22:457
9. Fan B, Fan W, Li R (2003) J Mol Chem A 201:137
10. Jin C, Fan W, Jia Y, Fan B, Ma J, Li R (2006) J Mol Chem A 249:23
11. Kervinen K, Bruijnincx PCA, Beale AM, Mesu JG, van Koten G, Gebbink RJMK, Weckhuysen BM (2006) J Am Chem Soc 128:3208
12. Mesu JG, Visser T, Beale AM, Soulimani F, Weckhuysen BM (2006) Chem Eur J 12:7167
13. Ribot F, Banse F, Sanchez C (1997) J Sol-Gel Sci Tech 8:529
14. Bareyt S, Piligkos S, Hasenknopf B, Gouzerh P, Lacôte E, Thorimbert S, Malacria M (2005) J Am Chem Soc 127:6788
15. Fu QJ, Steele AM, Tsang SC (2001) Green Chem 3:71
16. Laane J (1967) J Am Chem Soc 89:1144
17. Zhong S, Cheng Q, Li H (2003) Gaodeng Xuexiao Huaxue Xuebao 24:125
18. Camblor MA, Corma A, Perez-Pariente J (1993) J Chem Soc Chem Commun 557
19. Nakajima K, Tomita I, Hara M, Hayashi S, Domen K, Kondo JN (2005) Adv Mater 17:1839
20. Holmes RR (1989) Acc Chem Res 22:190
21. Banse F, Ribot F, Tolédano P, Maquet J, Sanchez C (1995) Inorg Chem 34:6371
22. Chaudhari K, Das TK, Rajmohanan PR, Lazar K, Sivasanker S, Chandwadkar AJ (1999) J Catal 183:281
23. Samanta S, Mal NK, Manna A, Bhaumik A (2004) Appl Catal A Gen 273:157
24. Cornelius M, Hoffmann F, Fröba M (2005) Chem Mater 17:6674
25. Sayari A, Wang W (2005) J Am Chem Soc 127:12194
26. Sakakura T, Choi J, Saito Y, Sako T (2003) Polyhedron 19:573